

Original

Steglich, D.; Tian, X.:

Prediction of Crashworthiness for extruded Magnesium Materials
Key Engineering Materials, Material Forming ESAFORM 2015 (2015)
Trans Tech Publications

DOI: [10.4028/www.scientific.net/KEM.651-653.1009](https://doi.org/10.4028/www.scientific.net/KEM.651-653.1009)

Prediction of Crashworthiness for extruded Magnesium Materials

D. Steglich^a, X. Tian^b

Institute of Materials Research, Materials Mechanics / ACE-Centre, Helmholtz-Zentrum
Geesthacht, Max-Planck-Str. 1, D-21502 Geesthacht, Germany

^adirk.steglich@hzg.de ^bxiaowei.tian@hzg.de

Keywords: magnesium extruded alloys; finite element analysis; compression; buckling; energy

Abstract. To assess the crashworthiness of simple wrought magnesium structures, the axial deformation behaviour of different square tubes produced from magnesium alloys AZ31 and ZE10 were numerically investigated under quasi-static compressive loading conditions. Finite-element simulations were conducted to predict and assess the plastic buckling and crush behaviour. The necessary data to determine parameters for the plastic potential were taken from compression tests conducted along different orientations. The yield function Hill48 was selected, despite its inability to capture the strength differential effect. The modelling approach pursued is justified by considering the mechanical loading conditions, the fabrication process of the profiles and its implication on strain anisotropy, balancing achievable accuracy and computational efforts. The simulation results revealed that the material work hardening rates evidenced in uniaxial compression tests influenced the buckling modes as well as the energy dissipation.

Introduction

Design and production of structural components for vehicles are challenging tasks, involving the development of alloys and manufacturing processes, the structural design, and the subsequent crashworthiness analysis. Finite element analyses are commonly used in this context to reduce the time needed to develop a new product. An accurate description of material behaviour is essential to obtain reliable results from such analyses. For structural components in passenger cars in general, manufacturers need to prove energy absorption and structural integrity in case of crash scenarios. Several criteria are used to assess crashworthiness prospectively, including the deformation pattern of the vehicle sub-structure, the acceleration experienced by the vehicle during impact, and the probability of injury predicted by human body models. The amount of energy dissipated during a crushing event is used to assess the crashworthiness of a structure.

In early analytical studies, the material behaviour of such a structure was assumed to be ideally plastic, which gave reasonably good predictions for monolithic aluminium and steel structures. Magnesium and its alloys as structural material came into focus recently. Its high specific strength may help to improve the fuel efficiency of vehicles. Depending on the processing route of the alloy (cast or wrought material), the resulting mechanical behaviour can be significantly different. In rolled sheets or extruded rods the crystallographic texture causes anisotropy and different yielding in tension and compression, referred to as the strength differential (SD) effect [1]. In contrast, in cast products the anisotropy and the SD effect are not pronounced. On the other side, wrought products might be preferred for structural components due to their superior ductility. This holds in particular true if the crashworthiness of structures is considered.

Thus, any analysis of the crushing and buckling behaviour of profiles obviously has to incorporate the different characteristic in tension and compression. Recent contributions in this field address the strain rate sensitivity of rolled sheets in tension [2, 3], the energy absorption behaviour of die cast alloys, e.g. [4], the failure pattern of extruded magnesium rods in axial compression [5] and FE-modelling of the response during axial crushing and 4-point bending [6].

The purpose of the study reported here is to investigate the performance of hollow rectangular extruded profiles produced from magnesium alloys AZ31 and ZE10, respectively, under quasi-static macroscopic compressive axial loading. Numerical predictions of the crushing behaviour are validated against mechanical tests. The dissipated energy leading to a collapse of the configurations

is evaluated from the simulations. This allows evaluating the potential of the magnesium profiles to guarantee or enhance their crashworthiness.

Materials and mechanical characterisation

Two different commercial magnesium alloys were selected for investigation: A well-known and widely used alloy AZ31 (Mg + 3%Al + 1%Zn) and an alloy, ZE10 (Mg + 1%Zn + 0.3%Ce based mischmetal), which offers an improved formability compared to AZ31 (shown e.g. in [7]). Furthermore, ZE10 used in this study shows improved ductility at room temperature compared to AZ31 which is associated with an effect of the included rare earth elements in ZE10 and the result of deformation and recrystallization during sheet rolling, see e.g.[8].

Indirect extrusion performed at the Extrusion Research Centre of TU Berlin was used to obtain hollow profiles with quadratic cross section (square tubes, 49 mm * 49 mm outer width, 1.7 mm wall thickness). Compression test samples from plane sections of the profiles were machined and stacked as suggested in [9, 10]. This allows uniaxial in-plane compression testing while avoiding buckling of the sample. Respective tests were conducted along the extrusion direction (ED) and perpendicular to the extrusion direction (TD). Extensometers were used to monitor the width change during compression, from which the accumulated r-value (strain anisotropy parameter) under the assumption of isochoric plastic deformation can be calculated. The extracted stress-strain curves and the r-values are given in Fig. 1. They show the sigmoidal shape typical for twinning-dominated deformation. Note that the stress level of ED and TD is reversed between the two materials.

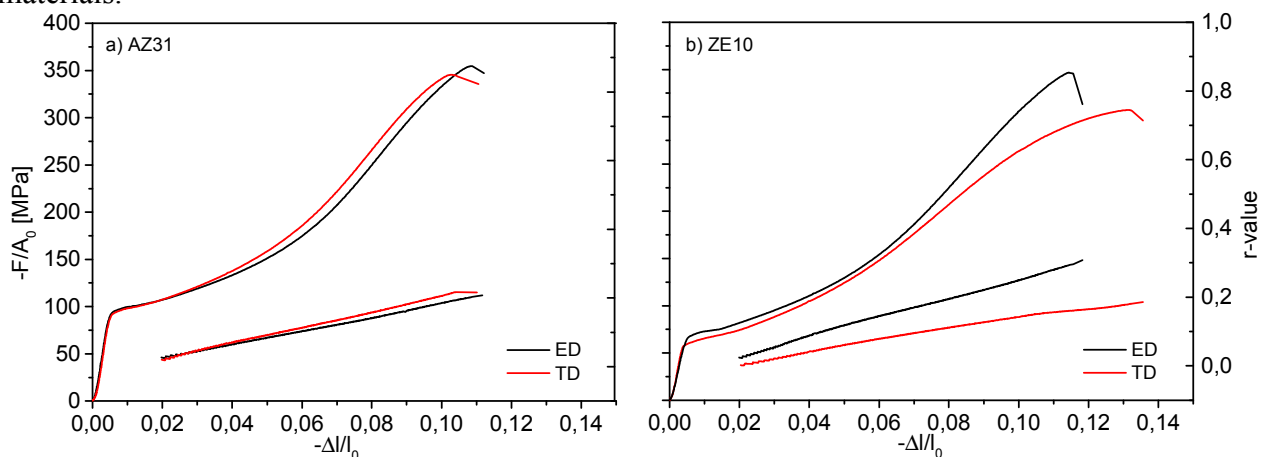


Fig. 1: Engineering stress – strain curves and (accumulated) r-value evolutions obtained from compression tests of AZ31 (a) and ZE10 (b)

Constitutive law

In view of forming and crushing applications a robust constitutive model accounting for elastic/plastic deformations is required. For materials with cubic crystal structure, phenomenological models based on orthotropic yield functions that capture both the anisotropy of yielding and the anisotropy of the r-value were proposed for this purpose (e.g. by Hill [11], Barlat et al. [12], Bron and Besson [13]). For hexagonal metals like magnesium, plastic potentials additionally accounting for the strength mismatch were developed, e. g. by Cazacu et al. [14]. The accuracy of predictions based on these models can be impressive; unfortunately they require not only high testing efforts to calibrate their parameters, but also the coding and the linking to the FE-solver.

In this light, an alternative way was trod here. In an attempt to minimise simulation time and parameter calibration efforts, Hills plastic potential was used together with an isotropic hardening law extracted from compression tests of the respective materials. Hills potential is implemented in the FE-code ABAQUS, therefore it is computationally more efficient compared to a user code. Second, the determination of Hills parameters is straight forward and therefore easy.

A yield surface describing the plastic state of a material is commonly defined by

$$\bar{\sigma} - R(p) = 0, \quad (1)$$

with $R(p)$ representing the flow stress as a function of the plastic equivalent strain describing the hardening of the material. Hill postulated that an equivalent stress is defined by

$$\bar{\sigma} = \sqrt{\frac{1}{2} \left[F(\sigma_{22} - \sigma_{33})^2 + G(\sigma_{33} - \sigma_{11})^2 + H(\sigma_{11} - \sigma_{22})^2 + 2L\sigma_{23} + 2M\sigma_{13} + 2N\sigma_{12} \right]}. \quad (2)$$

The six constants F, G, H, L, M, N describe the plastic anisotropy. In case of a plane stress conditions in the (1,2)-plane, four parameters F, G, H, N have to be calibrated.

From compression tests in the two orientations of orthotropy the constants F, G and H can be determined by considering the yield stress ratio and the r -value. The parameters used read $F=0.78, G=0.78, H=0.22, N=1.4$ for AZ31, and $F=1.08, G=0.85, H=0.15, N=1.24$ for ZE10. Fig. 2a illustrates the resulting yield surfaces, normalised by the yield stress along the ED. Note that the biaxial compressive yield stress is significantly lower in case of both materials compared to the von Mises yield criterion. This is a consequence of the small r -values in compression served as an input. The hardening function $R(p)$ was calculated from the compression test along the ED. A strain rate sensitivity – albeit considered in many contributions addressing dynamic impact – was not implemented here as the tests to simulate were of quasi-static nature. Isotropic hardening was considered for all the materials investigated.

Material failure was addressed by a phenomenological damage model, which is based on a critical (equivalent) failure strain defined as a function of the applied stress [15]. The dependency is expressed using the shear stress ratio Θ_s ,

$$\Theta_s = \frac{\bar{\sigma} - \frac{k_s}{3} \text{Tr}(\mathbf{S})}{\tau_{\max}}, \quad (3)$$

where $\bar{\sigma}$ is the equivalent stress defined in Eq. 2, as a function to the stress tensor's trace. τ_{\max} is the maximum shear stress and k_s is a model parameter, $k_s=0.3$.

The damage initiation function was calibrated based on the equivalent failure strain in uniaxial tension ($\Theta_s=1.8$) and uniaxial compression ($\Theta_s=2.2$). The equivalent failure strain in uniaxial compression is taken from the uniaxial compression test results, see Fig. 1. The respective value for uniaxial tension does not affect the structural response, which is primarily exposed to compressive stresses. However, it was set to $\varepsilon_f=0.18$ for AZ31 and 0.19 in case of ZE10. The displacement leading to final failure of a material point associated with a typical element size of 3 mm was selected to be 0.25 mm for both materials.

FE-simulations

Sections of 400 mm length (slender bars, length/width=8 [16]) were cut from the extruded profiles and subjected to a compressive axial displacement in a universal testing machine. The required force was recorded. The normalised crushing force (force divided by net cross section of the profile) as a function of the imposed displacement can be used to evaluate the profile's performance during this crush event. In case of the experiment conducted, the hollow profiles are centred on studs of 40 mm height and then clamped along their circumference. The FE-model of this test adopted the respective boundary conditions: the displacement components as well as all rotations were suppressed/prescribed. Linear shell elements were used for the profile's sides, see Fig. 2b. ABAQUS/Explicit was used for the simulations. In order to mimic the quasistatic process, mass scaling was adopted while controlling the kinetic energy to be less than 2% of the model's internal energy. For the FE-modelling of the crushing response, a geometrical imperfection was introduced by superimposing the first eigenmode on the initial configuration extracted from a preceding buckling analysis.

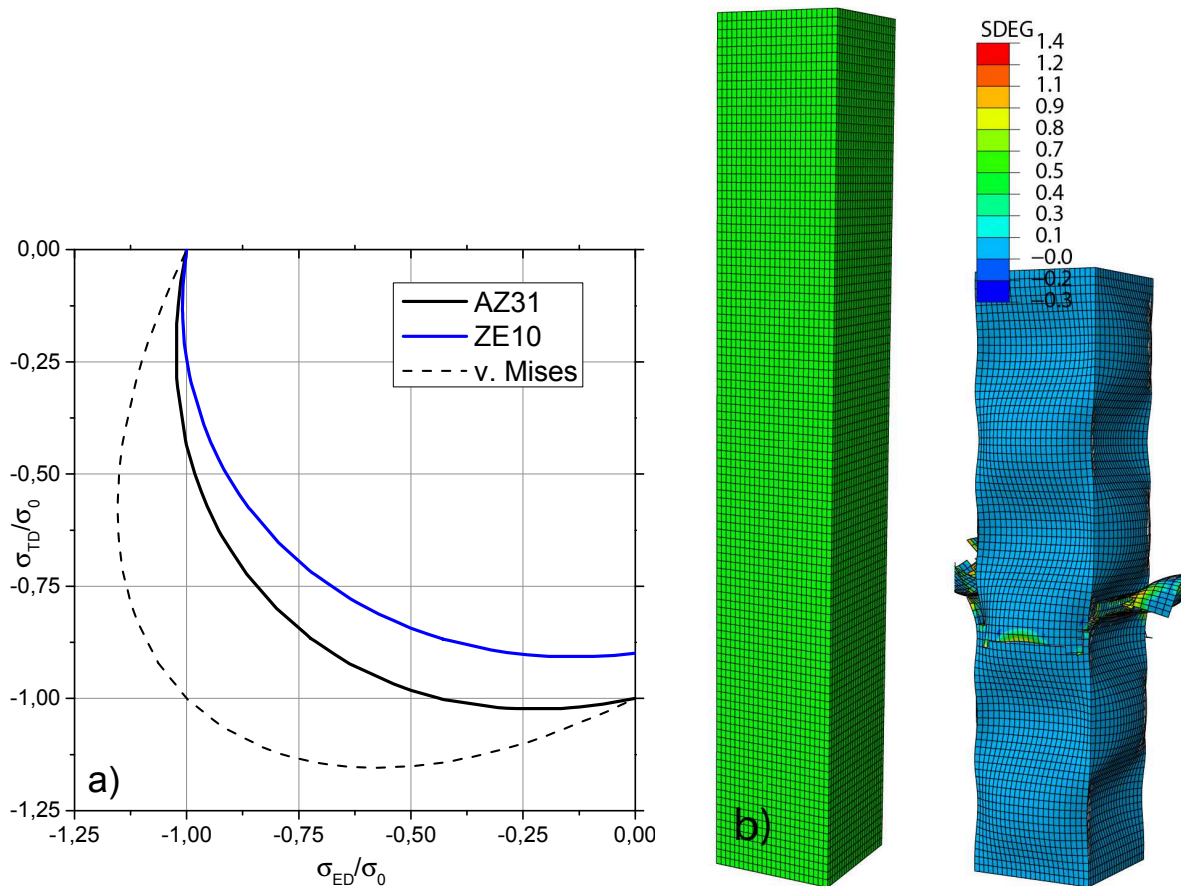


Fig. 2: a) plane stress representation of initial yield locus based on Hill48 yield function (3rd quadrant); b) undeformed and crushed extruded profile showing large segment failure – contours of constant stress degradation

Results

Fig. 3 shows the mechanical response of the square tubes during the crush test in terms of normalised force and specific plastic (dissipated) energy. At the early stage of deformation, a periodic buckling pattern was progressively established. Once one buckle was formed, it triggered its neighbour to evolve before cracks were initiated, see Fig. 2b, leading to a rise in the force level. At load maximum, cracks at the edges of the profile were initiated, leading to a sharp drop of the force. Once the axial displacement is further increased, shear-compression cracks will propagate mainly perpendicular to the loading direction. The simulations and the experiments reveal the same buckling modes and identical cracking pattern. While the experiments were stopped, the simulations predict large segment failure of the profile. The resulting stress carrying capacity is very small. In the final stage of compression, the predicted force increases due to jamming of broken parts. As this behaviour is strongly dependent on the boundary conditions of the test and appears as not reproducible in experiments, the assessment discussed in the following is based on a displacement of 60 mm.

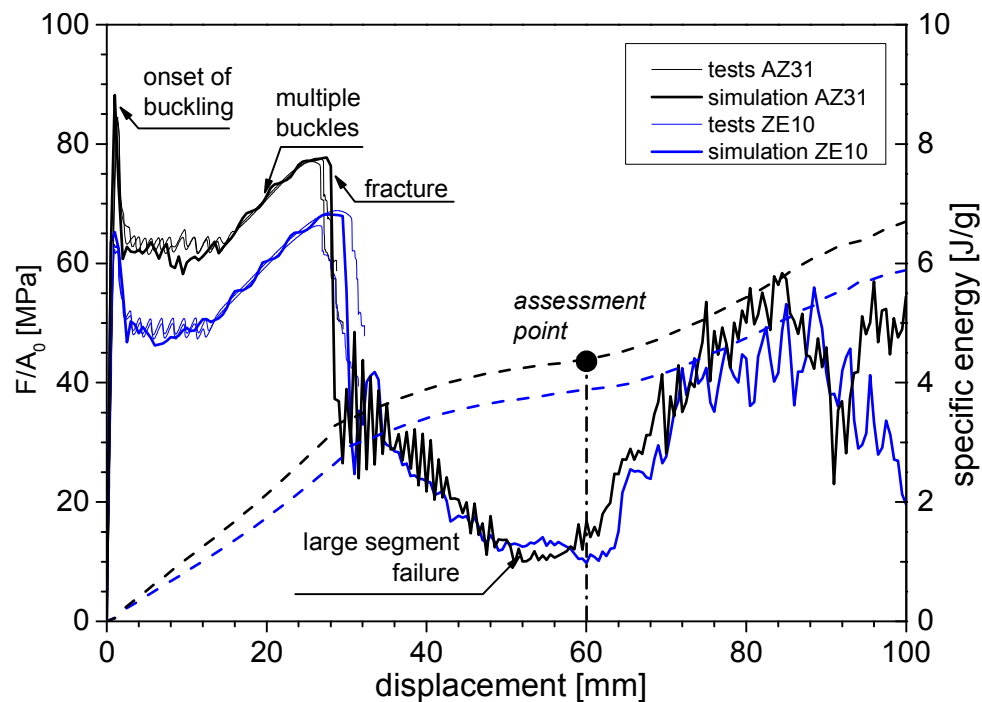


Fig. 3: Normalised force – displacement behaviour and specific plastic energy of the two square tubes during crushing

The specific dissipated energy was calculated based on the mass of the profile's deformed part, $m=188$ g. At a displacement of 60 mm, the respective energies read 4.4 J/g in case of AZ31, 3.9 J/g in case of ZE10. The slightly smaller value of ZE10 can be explained by the lower yield stress in compression compared to AZ31. Its improved ductility during tension (not shown here) cannot be exploited in the current loading scenario. Note that an equivalent aluminium profile (Al6060, same cross section, $m=311$ g) leads to an energy absorption of 4.8 J/g, which is in the same order of magnitude.

Conclusions

The crashworthiness of two magnesium alloys was assessed on the basis of finite-element simulations. Although it is worthwhile using advanced plastic potentials, it is shown here that a simple constitutive relation gives reasonably accurate results. This is directly related to the loading scenario (compressive load) considered and hence cannot be generalised. However, by considering the two main characteristics of the mechanical behaviour, namely compressive hardening and the low r -value, a "classical" plasticity model can be used. As damage initiation and evolution are considered, the method allows predicting the plastic and structural collapse of the tubes. While the profiles fracture into large segments, the authors suggest limiting the computation of the dissipated energy to a state at which the structures are still intact. Both, simulation and experimental results show a second force peak before failure together with a periodic buckling pattern, which contributes to the energy dissipation. This is related with the high hardening rates evidenced in uniaxial compression tests.

Acknowledgements

The authors like to thank Kay Erdmann for his kind assistance during mechanical testing and Jan Bohlen for providing insight into the material's microstructures. Support by the Assessment, Computing and Engineering Centre (ACE) and the Magnesium Innovation Centre (MagIC) of HZG is gratefully acknowledged. The authors furthermore appreciate the contributions of the Extrusion Research Centre of TU Berlin (Germany).

References

- [1] W.F. Hosford, T.J. Allen, Twinning and directional slip as a cause for a strength differential effect, *Metallurgical Transactions*, 4 (1973) 1424-1425.
- [2] D. Hasenpouth, C. Salisbury, A. Bardelcik, M.J. Worswick, Constitutive behavior of magnesium alloy sheet at high strain rates, in: *Dymat 2009*., Vol 2, E D P Sciences, 2009, pp. 1431-1435.
- [3] I. Ulacia, C.P. Salisbury, I. Hurtado, M.J. Worswick, Tensile characterization and constitutive modeling of AZ31B magnesium alloy sheet over wide range of strain rates and temperatures, *Journal of Materials Processing Technology*, 211 (2011) 830-839.
- [4] C. Dørum, O. Sture Hopperstad, O.-G. Lademo, M. Langseth, An experimental study on the energy absorption capacity of thin-walled castings, *International Journal of Impact Engineering*, 32 (2006) 702-724.
- [5] P.D. Beggs, W. Song, M. Easton, Failure modes during uniaxial deformation of magnesium alloy AZ31B tubes, *International Journal of Mechanical Sciences*, 52 (2010) 1634-1645.
- [6] F. Zhu, C.C. Chou, K.H. Yang, X. Chen, D. Wagner, S. Bilkhu, Application of AM60B magnesium alloy material model to structural component crush analysis, *International Journal of Vehicle Safety*, 6 (2012) 178-190.
- [7] M.N. Mekonen, D. Steglich, J. Bohlen, L. Stutz, D. Letzig, J. Mosler, Experimental and numerical investigation of Mg alloy sheet formability, *Materials Science and Engineering: A*, 586 (2013) 204-214.
- [8] J. Bohlen, M.R. Nuernberg, J.W. Senn, D. Letzig, S.R. Agnew, The texture and anisotropy of magnesium–zinc–rare earth alloy sheets, *Acta Mater.*, 55 (2007) 2101-2112.
- [9] D. Steglich, X. Tian, J. Bohlen, T. Kuwabara, Mechanical Testing of thin Sheet Magnesium Alloys in biaxial Tension and uniaxial Compression, *Experimental Mechanics*, 54 (2014) 1247-1258.
- [10] D. Ghaffari Tari, M.J. Worswick, U. Ali, M.A. Gharghour, Mechanical response of AZ31B magnesium alloy: Experimental characterization and material modeling considering proportional loading at room temperature, *International Journal of Plasticity*, 55 (2014) 247–267.
- [11] R. Hill, A theory of the yielding and plastic flow of anisotropic metals, *Proc. Roy. Soc. London A*, 193 (1948) 281-297.
- [12] F. Barlat, J.C. Brem, J.W. Yoon, K. Chung, R.E. Dick, D.J. Lege, F. Pourboghrat, S.-H. Choi, E. Chu, Plane stress yield function for aluminum alloy sheets-part 1: theory, *Int. J. Plast.*, 19 (2003) 1297-1319.
- [13] F. Bron, J. Besson, A yield function for anisotropic materials: Application to aluminium alloys, *Int. J. Plast.*, 20 (2004) 937-963.
- [14] O. Cazacu, B. Plunkett, F. Barlat, Orthotropic yield criterion for hexagonal closed packed metals, *Int. J. Plast.*, 22 (2006) 1171-1194.
- [15] H. Hooputra, H. Gese, H. Dell, H. Werner, A comprehensive failure model for crashworthiness simulation of aluminium extrusions, *International Journal of Crashworthiness*, 9 (2004) 449–463.
- [16] D. Steglich, X. Tian, J. Bohlen, S. Riekehr, N. Kashaev, K.U. Kainer, N. Huber, Experimental and numerical crushing analyses of thin-walled magnesium profiles, *International Journal of Crashworthiness*, (2015).